THE UNIVERSITY OF TEXAS AT DALLAS
McDermott Library

TREASURES
@UT Dallas

School of Natural Sciences and Mathematics

On the Diffusion Rates of Electron Bounce Resonant Scattering by Magnetosonic Waves

UT Dallas Author(s):

Armando A. Maldonado
Lunjin Chen

Rights:

©2018 American Geophysical Union. All Rights Reserved.

Citation:

Maldonado, Armando A., and Lunjin Chen. 2018. "On the diffusion rates of electron bounce resonant scattering by magnetosonic waves." Geophysical Research Letters 45(8): 3328-3337. doi:10.1002/2017GL076560

This document is being made freely available by the Eugene McDermott Library of the University of Texas at Dallas with permission of the copyright owner. All rights are reserved under United States copyright law unless specified otherwise.

Geophysical Research Letters

RESEARCH LETTER
10.1002/2017GL076560

On the Diffusion Rates of Electron Bounce Resonant Scattering by Magnetosonic Waves

Armando A. Maldonado[1] **and Lunjin Chen**[1]

[1]Department of Physics, University of Texas at Dallas, Richardson, TX, USA

Key Points:
- A generalized diffusion coefficient formula for the bounce resonance interaction between electrons and fast magnetosonic waves is presented
- Effective bounce resonance scattering is controlled by the strength of wave magnetic mirror forces with finite-Larmor-radius correction
- The dependence of bounce resonant diffusion coefficients on key parameters is presented and explained

Correspondence to:
A. A. Maldonado,
aam131130@utdallas.edu

Citation:
Maldonado, A. A., & Chen, L. (2018). On the diffusion rates of electron bounce resonant scattering by magnetosonic waves. *Geophysical Research Letters*, *45*, 3328–3337. https://doi.org/10.1002/2017GL076560

Received 26 NOV 2017
Accepted 19 FEB 2018
Accepted article online 28 FEB 2018
Published online 19 APR 2018

Abstract Magnetosonic waves have been demonstrated as effective for bounce resonant scattering. Electron scattering rates due to bounce resonance interaction with magnetosonic waves are derived in a general form, where the effects of the finite Larmor radius, of violation in the first adiabatic invariant, and of latitudinal wave power distribution are considered. Such bounce resonance diffusion coefficients are important, but missing, from radiation belt modeling. Additionally, we provide a parametric study on the electron energy and equatorial pitch angle, magnetosonic wave, and background parameters to identify the factors that determine effective bounce resonant scattering.

Plain Language Summary Energetic particles, like electrons, emitted from the Sun become trapped in the Earth's magnetic field and form a complicated system of plasma currents known as the magnetosphere. Electrons in the magnetosphere move in ways that are difficult to model. Understanding the behavior of energetic particles in the plasma of the magnetosphere is important for planning both manned, and unmanned, space missions. Typically, there are many waves and particles in the magnetosphere, so identifying and studying each interaction makes modeling a complete magnetosphere possible. Magnetosonic waves are plasma waves that disturb electrons in ways that previous theories could not predict, but data have always shown. In this study, we use our own model to look at the spread of many electrons, bouncing along the magnetic field lines, after encountering multiple magnetosonic waves. It was found that considering the radius of the gyration of the particle and a realistic geometry of the wave are important to the outcome of the interaction. The spread of the particles is called diffusion and can be used in larger-scale models to better predict the dynamics of the magnetosphere as a tool to help plan future space missions.

1. Introduction

Fast magnetosonic waves (ion Berstein mode waves or equatorial noise) are magnetically compressional mode electromagnetic waves observed within a few degrees of the geomagnetic equator. They can be observed over a frequency range of a few hertz to a few hundred hertz but are bounded by the proton gyrofrequency (f_{ch}) and lower hybrid resonance frequency (f_{LHR}, Russell et al., 1969). Fast magnetosonic waves also propagate nearly perpendicular to the background magnetic field and are generated at harmonics of the proton gyrofrequency through ion cyclotron harmonic instability of energetic proton ring distributions with energy of ~10 keV (Boardsen et al., 1992; Chen et al., 2010; Horne et al., 2000; Liu et al., 2011). The condition of transition from discrete to continuous frequency spectra has been investigated thoroughly (Sun et al., 2016a, 2016b). It is also observed that their dominant magnetic component points along the field line and has an average amplitude of about 50 pT (Ma et al., 2013) and can be as high as 1 nT (Tsurutani et al., 2014).

Both bounce and Landau resonant scattering by magnetosonic waves have been attributed to the formation of butterfly distributions, which require a depletion in equatorially and near equatorially mirroring electrons and/or enhancements for lower pitch angled electrons (Li et al., 2016; Ma et al., 2016; Maldonado et al., 2016; Xiao et al., 2015). Recent attempts to recreate this electron population distribution have involved scattering by magnetosonic waves through Landau resonance and transients time scattering effects (Li et al., 2016; Ma et al., 2016) and from the combined acceleration of magnetosonic waves and chorus waves through violation of the first adiabatic invariant (Xiao et al., 2015). Although these studies found the formation of butterfly distributions to be on the order of minutes and hours, respectively, such formations were observed to occur

©2018. American Geophysical Union. All Rights Reserved.

within seconds and comparable phase space density distributions were produced by simulating Landau and bounce resonance with fast magnetosonic waves (Maldonado et al., 2016).

Nonlinear bounce resonance of energetic, equatorially mirroring electrons with monochromatic magnetosonic waves has been studied in Chen et al. (2015) through test-particle simulations. Diffusion rates of this interaction are desired for future studies and have been attempted in the past but only for nonequatorially mirroring pitch angles $\alpha_{eq} < 90°$ (Li et al., 2015; Shprits, 2016). Li et al. (2015) follows the method of Roberts and Schulz (1968) and Schulz and Lanzerotti (1974) by assuming a guiding center approximation (motion of the gyrocenter of the particle) and a flat power distribution over a specified magnetic latitude range. Later studies adapted Li et al.'s (2015) model to explore the effect of multiple waves with normally distributed wave normal angles (Li & Tao, 2018; Tao & Li, 2016). Two potentially important factors, however, have been ignored for bounce resonant scattering rate evaluation. The first one is that the wavelength of those magnetic waves can be comparable to, and shorter than, the gyroradius of energetic electrons, especially for radiation belt electrons. As a consequence, the first adiabatic invariant can be violated and the net force of magnetosonic wavefields can be considerably different from using a guiding center approximation, where the gyroradius is assumed to be much smaller than the wavelength. The second factor is that the observed latitudinal wave power distribution shows a narrow peak near the equator instead of being flat (Němec et al., 2005). These factors are valuable for quantifying the effect of magnetosonic waves on electron scattering. In this study, we put forward a general bounce resonant scattering model, which implements the previously mentioned factors, and then validate it against test-particle simulation results. A parametric study of various particle, wave, and background parameters are also presented to explore effective scattering conditions between energetic electrons and magnetosonic waves.

2. Derivation of Diffusion Coefficients

Formulation of the bounce resonance diffusion coefficients utilizes a set of gyro-averaged relativistic particle equations from Bortnik and Thorne (2010) and Chen et al. (2015). The set of equations considers a relativistic guiding center approach, multiple waves, the Larmor radius effect, and a Gaussian latitudinal profile for the magnetosonic wave amplitude.

$$\frac{dp_z}{dt} = -\frac{p_\perp^2}{2\gamma mB}\frac{dB}{ds} + g(\lambda)\sum_n \left[e^{i\phi_n}\frac{qE_{zn}J_0(\beta_n) + iqv_\perp B_{xn}J_{+1}(\beta_n)}{2} + \text{c.c.}\right] \tag{1}$$

$$\frac{dp_\perp}{dt} = +\frac{p_z p_\perp}{2\gamma mB}\frac{dB}{ds} + g(\lambda)\sum_n \left[e^{i\phi_n}\frac{-iqE_{yn} - iqv_z B_{xn}}{2}J_{+1}(\beta_n) + \text{c.c.}\right] \tag{2}$$

$$\frac{d\phi_n}{dt} = -\omega_n + k_{zn}v_z \tag{3}$$

Here m is the electron's mass, γ is the Lorentz factor, and p_z (v_z) and $p_\perp$ ($v_\perp$) are the particle's parallel and perpendicular momentum (velocity), respectively. Our background field B is assumed to be dipolar, and s is the arc distance along the field line from the geomagnetic equator. E_{zn}, B_{xn}, and E_{yn} are the nth magnetosonic wavefield components, which are given in the field-aligned coordinate system where z is along the background field, the x-z plane contains the wave vector $\vec{k}$, and y completes the right-handed coordinate system. The terms $J_0(\beta)$ and $J_{+1}(\beta)$ are Bessel functions of the first kind with argument $\beta_n = \frac{k_{\perp n}p_\perp}{qB}$, where n denotes the nth wave, $k_\perp$ is the perpendicular wave number, and q is the charge (with sign) of an electron. The c.c. terms represent the complex conjugate of the displayed wave force terms. These Bessel terms arise due to the wave phase variation along the gyromotion path, which is also known as the finite Larmor radius effect. It should be pointed out that $|J_0(\beta)| < 1$ and $|J_{+1}(\beta)| < \beta/2$ produce a smaller driving force than the typical guiding center approximation which ignores the size of the Larmor radius. Equations (1) and (2) can be reduced to the guiding center approximation by letting β approach 0. The additional factor $g(\lambda) = \exp(-\frac{\lambda^2}{\Delta\lambda^2})$ represents a realistic latitudinal distribution of the wave amplitude, where λ is the geomagnetic latitude from the geomagnetic equator. The term ϕ_n in equation (3) is the nth wave phase seen by the center of the gyromotion, where ω_n is the nth wave's angular frequency and k_{zn} is the corresponding field-aligned wave vector component.

We present a summary of the derivation of diffusion coefficients for our wave model below with a detailed derivation in Appendix A. We begin by finding the change in the squared momentum, Δp^2, and the magnetic

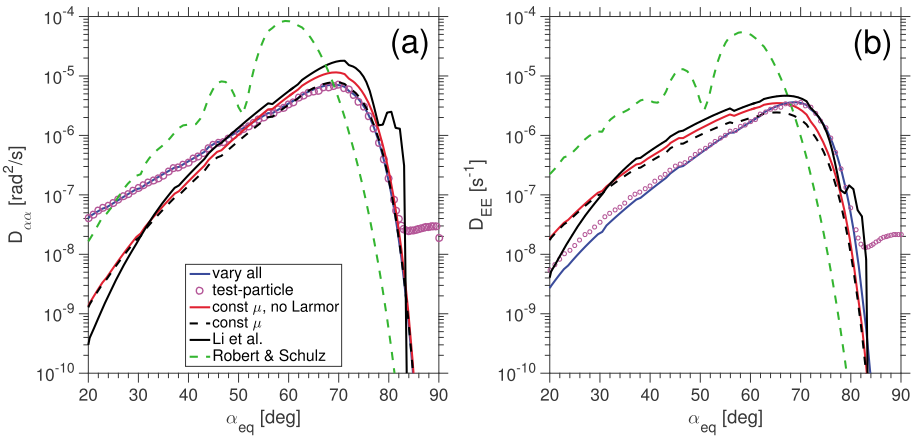

Figure 1. Comparison of (a) pitch angle and (b) energy diffusion coefficients among our new analytical expression, Robert and Schulz theory (Li et al., 2015), the formula under the assumption of zero Larmor radius, the formula under the assumption of the magnetic moment conservation, and lastly the test-particle simulation results.

moment associated with the gyromotion, $\Delta\mu$, over a bounce period, τ_b, which are determined from our starting equations (1) and (2). Note that the magnetic moment is $\mu = \frac{p_\perp^2}{2mB}$ where m is the electron's mass and B is the background magnetic field at the particle's position in space.

$$\Delta p^2 = \sum_n \tau_b e^{(i\phi'_{n0})} \sum_{l_1} \sum_{k_2} J_{l_1}(k_{zn} z_m) I_{k_2}(c_0) e^{-c_0} \times \left[(-iqE_{yn} J_{+1} p_\perp) \frac{1}{2} \delta(l_1 - x_n \pm 2k_2) + (\gamma m z_m \Omega_b q E_{zn} J_0) \frac{1}{4} \delta(l_1 - x_n \pm 2k_2 \pm 1) \right] + \text{c.c.} \tag{4}$$

$$\Delta\mu = \sum_n \tau_b e^{(i\phi'_{n0})} \sum_{l_1} \sum_{k_2} J_{l_1}(k_{zn} z_m) I_{k_2}(c_0) e^{-c_0} \times \left[\left(-i \frac{\mu}{p_\perp} q E_{yn} J_{+1} \right) \frac{1}{2} \delta(l_1 - x_n \pm 2k_2) + \left(i \frac{\mu}{p_\perp} q z_m \Omega_b B_{xn} J_{+1} \right) \frac{1}{4} \delta(l_1 - x_n \pm 2k_2 \pm 1) \right] + \text{c.c.} \tag{5}$$

where $c_0 = \lambda_m^2 / 2\Delta\lambda^2$, $x_n = \omega_n / \Omega_b$, and Ω_b is the bounce frequency of the particle. For c_0, λ_m is the bounce mirror point as the magnetic latitude. The term $\delta(l_1 - x_n \pm 2k_2) = \delta(l_1 - x_n + 2k_2) + \delta(l_1 - x_n - 2k_2)$. Similarly, $\delta(l_1 - x_n \pm 2k_2 \pm 1) = \delta(l_1 - x_n + 2k_2 + 1) + \delta(l_1 - x_n - 2k_2 + 1) + \delta(l_1 - x_n + 2k_2 - 1) + \delta(l_1 - x_n - 2k_2 - 1)$. From here we are able to express the equatorial pitch angle change, $\Delta\alpha_{eq}$, and energy change, ΔE, in terms of Δp^2 and $\Delta\mu$.

$$\Delta\alpha_{eq} = \frac{1}{2} \tan(\alpha_{eq}) \left(\frac{\Delta\mu}{\mu} - \frac{\Delta p^2}{p^2} \right) \tag{6}$$

$$\Delta E = \frac{\Delta p^2}{2\gamma m} \tag{7}$$

To solve for the diffusion coefficient, D_{aa} (where a can be either α_{eq} or E), we write the change over a bounce period in the form $\Delta a = \tau_b \exp(i\phi'_{n0}) A + \text{c.c.}$, where A is a complex number independent of ϕ_{n0} and θ_0. The diffusion coefficient is

$$D_{aa} = \left\langle \frac{(\Delta a)(\Delta a)}{2\tau_b} \right\rangle = \frac{\tau_b}{2} (AA^* + A^* A) \tag{8}$$

where $\langle\rangle$ represents the average over the bounce phases θ_0 or wave phases ϕ_{n0}. Note that the quantity A in equation (8) is independent of the wave phase, ϕ_{n0}, and is linearly dependent on the wave's complex amplitudes E_{zn}, B_{xn}, and E_{yn} and contain the derived harmonic selective terms $\delta(l_1 - x_n \pm 2k_2)$ and $\delta(l_1 - x_n \pm 2k_2 \pm 1)$. Since the mirror point (λ_m and z_m) depends on α_{eq}, $D_{\alpha_{eq}\alpha_{eq}}$, and D_{EE} are individually calculated for each desired equatorial pitch angle.

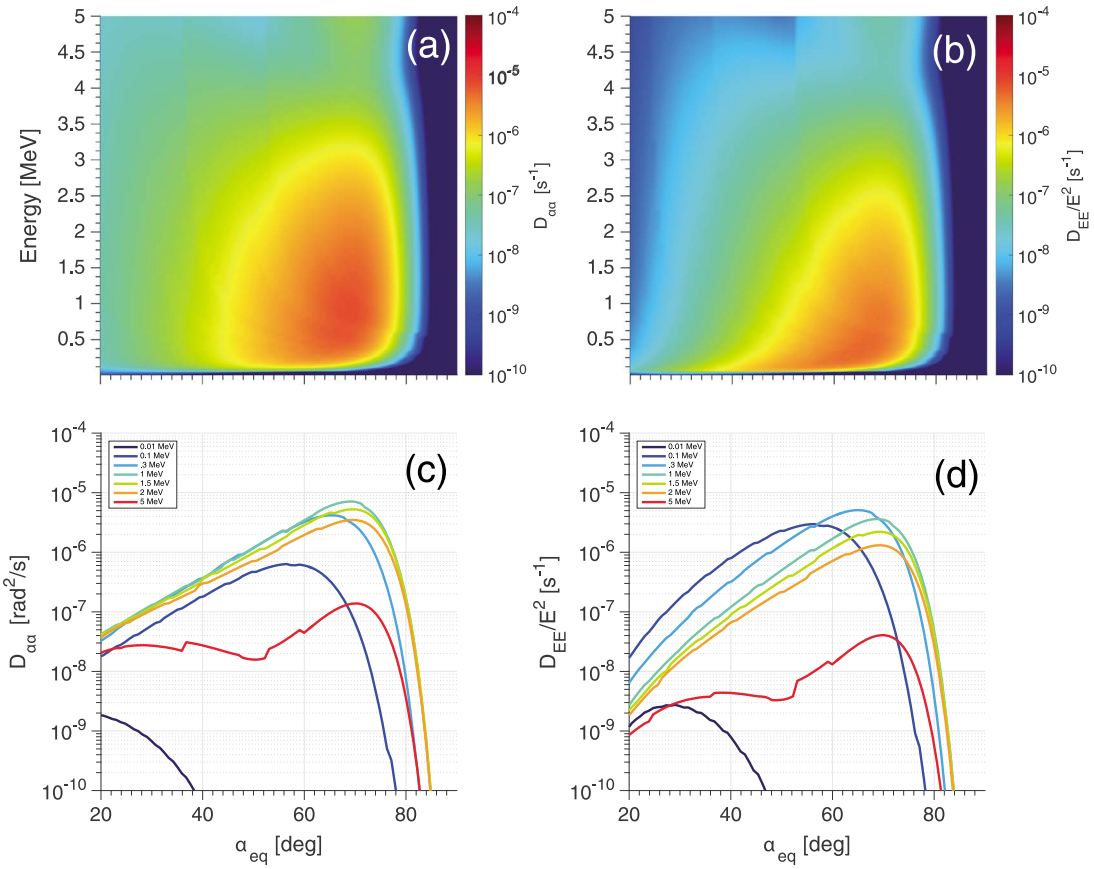

Figure 2. Pitch angle (a) and energy (b) diffusion coefficients as a function of equatorial pitch angle α_{eq} and energy. Pitch angle (c) and energy (d) diffusion coefficients for selected particle energies of 0.01, 0.1, 0.3, 1, 1.5, 2, and 5 MeV.

3. Test-Particle Simulation and Results

A test-particle simulation was completed using the same model given in the previous section. The simulation is carried out in a cold plasma contained in a background dipole magnetic field. Our magnetosonic power distribution follows the model from Horne et al. (2007) where the spectral density is $\mathcal{B}(\omega) \propto \exp(-(\omega - \omega_m)^2/\delta\omega^2)$. We follow Horne et al. (2007) and X. Li et al. (2015)'s wave parameters where $B_{rms} = 218$ nT, $\omega_m = 3.49 \times 10^{-3}\Omega_e$, and $\delta\omega = 8.86 \times 10^{-4}$. The bounds of the spectral density distribution are between $\omega_{LC} = 2 \times 10^{-3}\Omega_e$ and $\omega_{UC} = 5 \times 10^{-3}\Omega_e$, where Ω_e is the electron cyclotron frequency. The electron's kinetic energy is $E = 1$ MeV, with a drift shell of $L = 4.5$ and background plasma density $f_{pe}/f_{ce} = 3$. This will emulate electrons in the outer radiation belt outside of the plasmapause. Additionally, we assume that the waves have the same wave normal angle of $\psi = 89°$ and the latitudinal distribution has a latitudinal width of $\Delta\lambda = 3°$.

The simulation is performed for 100×101 runs over an interval of $t = 5$ s (~10 bounce periods) with 101 random wave phases and 100 random bounce phases. For a given α_{eq}, and E, for each run, we evaluate the change $\Delta\alpha_{eq}$ and ΔE over the simulation time t. We evaluate the equatorial pitch angle diffusion coefficient through $D_{\alpha_{eq}\alpha_{eq}} = \left\langle (\Delta\alpha_{eq})^2 \right\rangle / 2t$, where $\Delta\alpha_{eq} = \alpha_{eq} - \alpha_0$ is the change in equatorial pitch angle from the original value, t is the simulation time and $\langle\rangle$ is an ensemble average over the bounce phases θ and wave phases ϕ_{n0}. Test-particle simulation results are shown as the pink circles in Figure 1, and we refer to the blue line for our analytical results. One can see that our test-particle simulation (pink circles) is in close agreement with our theoretical derivation with an exception for pitch angles near 90°. There are two reasons for the discrepancy. The first is that our assumption of zeroth-order bounce trajectory used in the linear perturbation analysis fails near 90°. In other words, for equatorially mirroring electrons, any small perturbation results in a significant change to the bounce amplitude. This requires nonlinear analysis (e.g., Chen et al., 2015) to capture the response of equatorially mirroring electrons, where advective transport in the pitch angle and energy for those electrons should be considered. The second is associated with errors from numerical integration

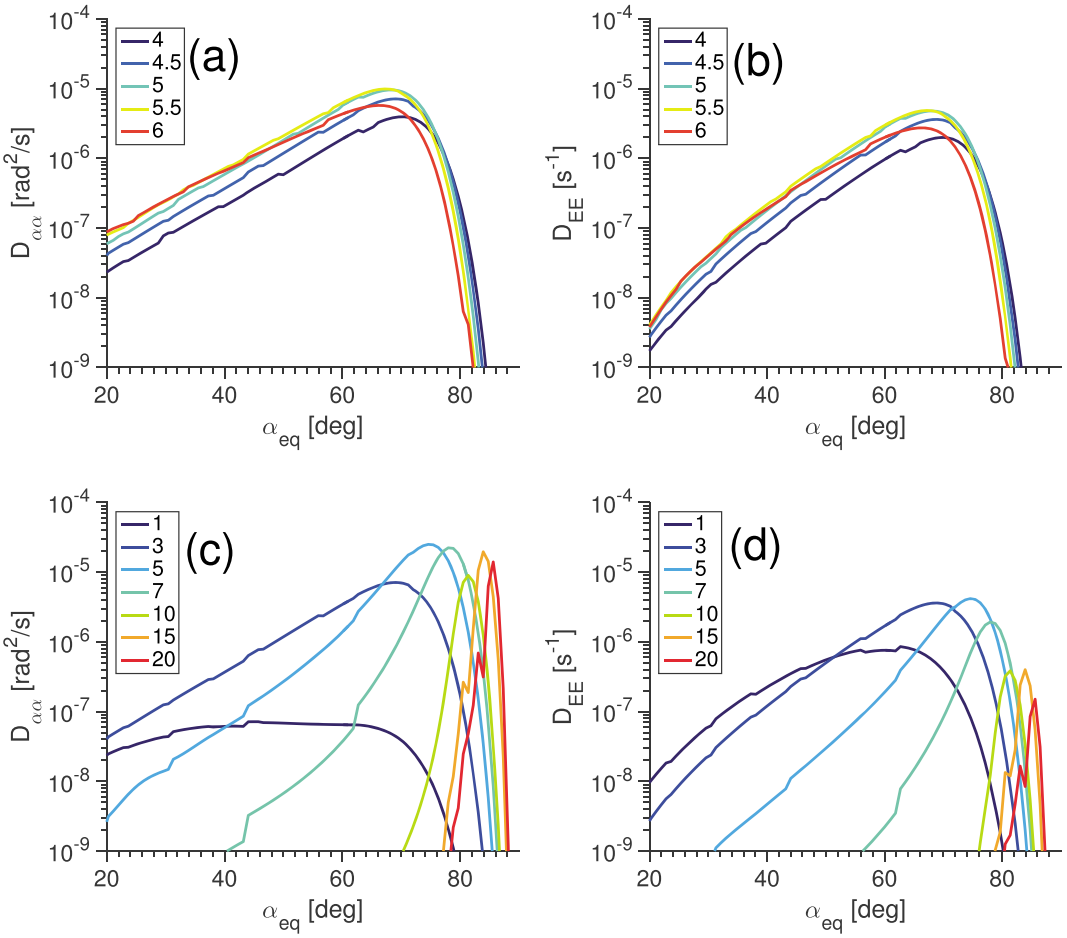

Figure 3. Pitch angle (a) and energy (b) diffusion coefficients as a function of equatorial pitch angle α_{eq} for selected L values: 4, 4.5, 5, 5.5, and 6. Pitch angle (c) and energy (d) diffusion coefficients for selected values of plasma frequency to cyclotron frequency ratios (f_{pe}/f_{ce}) of 1, 3, 5, 7, 10, 15, and 20.

in the test-particle simulations. Because of the absence of nonlinear effects in our linear perturbation analysis, we believe diffusion rates near $\alpha_{eq} = 90°$ to be more reliable for our test-particle simulations than our analytical result.

For comparison, we also calculate two other analytical diffusion rates (red line and black dashed line) which both assume magnetic moment conservation, but differ in assuming an absent (red line) and present (black dashed line) Larmor radius effect. The diffusion rate derivation for the assumption of magnetic moment conservation (independent of finite size Larmor radius assumption) is done by letting the wave driving term in equation (2) vanish. The diffusion rate derivation for the assumption of zero Larmor radius is done by setting $J_0(\beta) = 1$ and $J_{+1}(\beta) = \beta/2$ in equations (1) and (2). The peak pitch angle scattering rate when including all effects (blue line) at large pitch angles is lower than those under the assumption of zero Larmor radius (red line). This is because the Larmor radius effect ($J_0(\beta)$ and $J_{+1}(\beta)$ in equations (1) and (2) reduces the scattering of magnetosonic waves on our electron population. Including Bessel functions tend to reduce the strength of the wave driving force (if $\beta > 1$, $J_0(\beta) < 1$ and $J_{+1}(\beta) < \beta/2$) and therefore reduce the driving force effect. A significant difference between our analytical results (blue line) and those with the assumption of magnetic moment conservation (dashed black line) exists at small pitch angles (<40°). This is expected because those electrons can travel through the wavefield quickly, and thus, the magnetic moment is not expected to be conserved.

We also make a comparison with the formula obtained from previous studies which do not incorporate the Larmor radius effect or any driving force to $p_\perp$. Diffusion rates from Roberts & Schulz (1968, flat latitudinal profile) and Li et al. (2015, square latitudinal profile) are shown as the green line and solid black line in Figure 1,

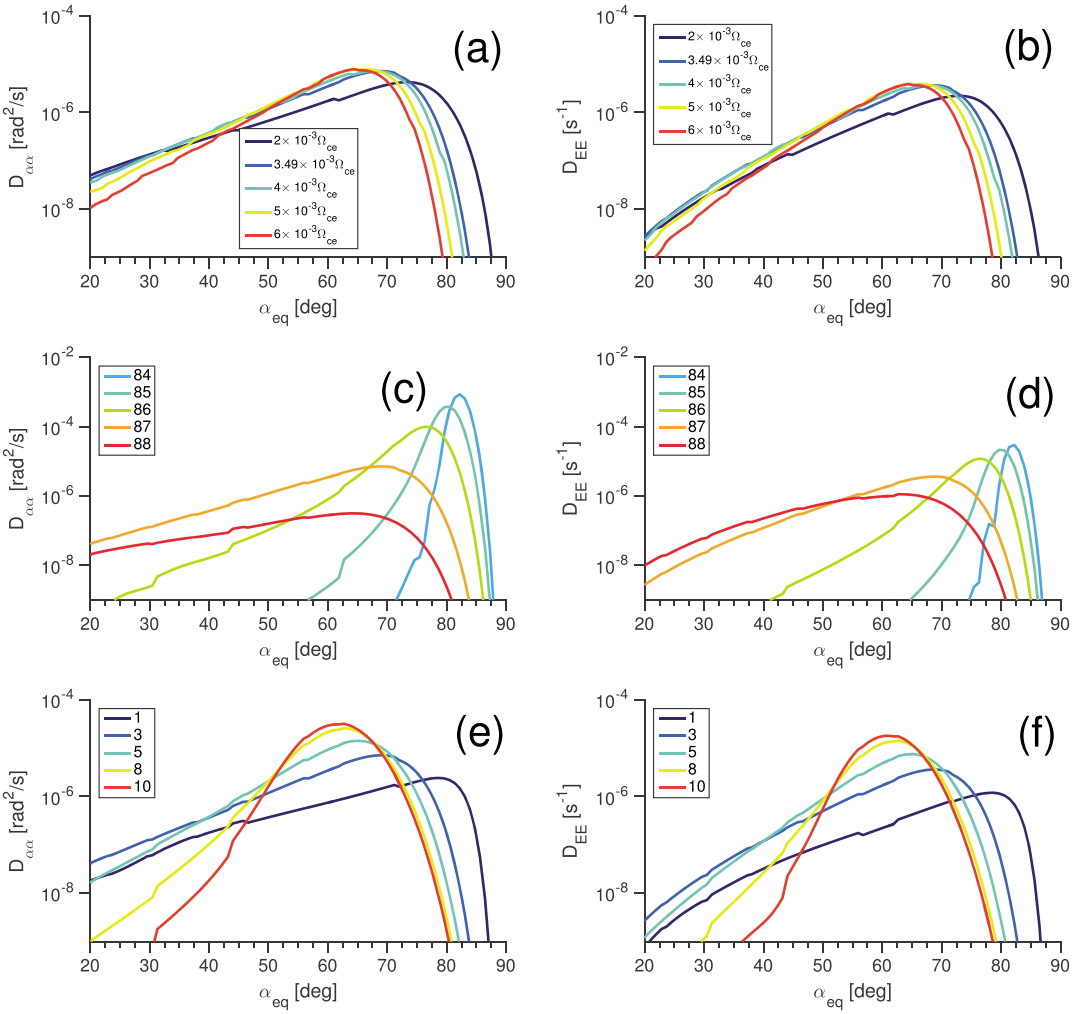

Figure 4. Pitch angle (a) and energy (b) diffusion coefficients as a function of equatorial pitch angle α_{eq} and for selected values of wave center frequencies. Pitch angle (c) and energy (d) diffusion coefficients for selected values of wave normal angles. Pitch angle (e) and energy (f) diffusion coefficients for selected values of latitudinal widths for the wave power distribution.

respectively. The two follow the same general trend as those from our formulation (the blue line). However, our formulation predicts a smaller pitch angle diffusion rate peak near high pitch angles (~70°) due to the same reasons mentioned above. One can also see discontinuities in the diffusion rates from Li et al. (2015) as a result of nonrealistic latitudinal distributions used for the wave's power.

4. Parametric Analysis

In this section, effective conditions for bounce resonant scattering are explored by examining the dependence of our analytical diffusion coefficient formula on key parameters, which include particle energy, L-shell, electron plasma-to-gyrofrequency ratio f_{pe}/f_{ce}, spectral wave density distribution center, wave normal angle, and latitudinal power distribution. The parametric study will be done by changing only one of the parameters at a time and keeping the rest unchanged. Our nominal parameter set, given in the last section, emulates electrons in the outer radiation belt outside of the plasmapause.

In Figure 2 the dependence of diffusion coefficients on the particle's energy is shown. Diffusion coefficients for different energies maximize at similar equatorial pitch angles, which is in part due to the weak dependence of bounce frequency on particle energy. The diffusion coefficients are significant for a limited range of energy.

For sufficiently small energy, the wave magnetic mirror force, which is the dominant wave force and is proportional to the magnetic moment, vanishes. For sufficiently high energy, the Larmor radius effect weakens the wave force strength.

The L-shell in Figures 3a and 3b varies from our nominal value of 4.5 to values of 4, 5, 5.5, and 6. Overall, the dependence on the particle's L-shell value is weak. In Figures 3c and 3d, the value of $f_{pe}/f_{ce} = 3$ was altered from this nominal value to ratios of 1, 5, 7, 10, 15, and 20. For increasing f_{pe}/f_{ce}, peak diffusion rates shift to higher pitch angles, which is due to the nature of our Bessel term, J_{l1} (equations (4) and (5)), in our derivation of the diffusion rates which is dependent on the wave vector component (k_{zn}) and magnetic mirror point (z_m) for the particle. In general, for a given order n, $J_n(k_{zn}z_m)$ maximizes at a fixed value of $k_{zn}z_m$. As f_{pe}/f_{ce} increases, k_{zn} increases (because of increasing refractive index). As a result, z_m (corresponding to the peak diffusion rate) decreases; that is, the pitch angle corresponding to the peak diffusion rate increases. Note that z_m decreases and approaches 0 as α_{eq} approaches 90°.

In Figures 4a and 4b, the dependence of diffusion coefficients on the center frequency of the power distribution is examined. As the center frequency increases, the peak diffusion coefficient shifts toward smaller pitch angle values. This is because lower harmonics are included in the diffusive interaction (as the center wave frequency decreases) which contributes to greater scattering for higher pitch angled particles, a fact also noted in Shprits (2016). As a consequence, the diffusion rate magnitude for pitch angles near $\alpha_{eq} = 90°$ becomes higher for lower centers of the frequency distribution.

In Figures 4c and 4d we examine the dependence on the wave normal angle. As the wave normal angle decreases from 90°, the peak diffusion rate becomes greater and shifts to higher pitch angles. Increasing the wave normal angle effectively reduces the peak diffusion rate which is expected. Wave magnetic mirror force strength increases with increasing k_{zn} (i.e., decreasing wave normal angle); the magnetic mirror term containing B_{xn} is proportional to $k_{zn}B_{zn}$ because $k_{\perp n}B_{xn} + k_{zn}B_{zn} = 0$. Decreasing the wave normal angle also increases the parallel wave vector k_{zn}, leading to a shift of peak diffusion rates to higher pitch angles for the same reason discussed concerning Figure 3c. In other words, decreasing the wave normal angle also leads to increased scattering for near equatorially mirroring electrons.

In Figures 4e and 4f we show the dependence on the latitudinal width of our wave amplitude distribution model. As the distribution becomes wider, the diffusion coefficients start to behave as if the wave's latitudinal distribution was flat (Figure 1a, green dotted line). This feature is expected since the latitudinal distribution begins to approach a flat distribution similar to Schulz and Lanzerotti (1974). The peak diffusion coefficient shifts to smaller pitch angles for the wider distribution. This arises due to the second summation term, I_{k2}, in equations (4) and (5) based on its dependence on the latitude width of the wave power. The maximum value of the modified Bessel factor I_{k_2} requires a fixed value of $c_0 = \lambda_m^2/2\Delta\lambda^2$. As the latitudinal width $\Delta\lambda$ increases, the peak diffusion coefficient corresponds to a greater value of λ_m, that is, a smaller equatorial pitch angle.

5. Conclusions and Discussion

We present a derivation of the bounce resonance diffusion coefficients for the interaction between magnetosonic waves and the bounce motion of energetic electrons. Such derivation takes into account the Larmor radius effect, violation of the magnetic moment, and a physical wave power distribution. The derived formula is later verified by test-particle simulation results. The dependence of bounce resonance diffusion coefficients on various parameters is investigated. Our principal conclusions can be summarized as follows:

1. We present a generalized diffusion coefficient formula for the bounce resonance interaction between electrons and magnetosonic waves. The Larmor radius effect reduces the effective pitch angle scattering rate by magnetosonic waves for large pitch angles. Violation of the magnetic moment μ is mainly important for pitch angle scattering of the lower pitch angles. Using a realistic latitudinal distribution of wave power in our formula also provides a smoother diffusion coefficient curve than the curves produced in Li et al. (2015).
2. The energy and pitch angle regime of the effective bounce resonance scattering by fast magnetosonic waves is generally controlled by the strength of wave magnetic mirror forces with finite Larmor radius correction.
3. Peak diffusion coefficients tend to shift toward an equatorial pitch angle of 90° as the ratio of f_{pe}/f_{ce} increases and center frequency, wave normal angle, and latitudinal wave power width decrease.

Additionally, electron bounce resonant scattering has been shown to be possible with H^+ band electromagnetic ion cyclotron (EMIC) waves and low-frequency hiss (Cao, Ni, Summers, Bortnik, et al., 2017; Cao, Ni, Summers, Zou, et al., 2017) and could be affected by the Larmor radius effect depending on propagation angle, plasma density, and other geomagnetic conditions. Our bounce resonance diffusion coefficients are comparable in magnitude to those due to cyclotron resonance such as chorus waves (Shprits et al., 2006). The parametric study was presented to reveal key parameters for nearly equatorially mirroring electron bounce resonant scattering by fast magnetosonic waves (or ion Bernstein mode waves), which can result in the formation of electron butterfly pitch angle distributions. One may expect that such scattering is favored when encountering the wave with low proton cyclotron harmonics inside the outer plasmasphere (large value of f_{pe}/f_{ce}), for example, the event reported by Maldonado et al. (2016). The scattering of nearly equatorially mirroring electrons is more effective for a smaller value of the incoming wave normal angle and the latitudinal width of the power distribution. However, one should note that the variation of wave normal angle is related to the latitudinal extension through wave propagation (Boardsen et al., 1992). As wave normal angle decreases, the wave can propagate toward higher latitude, which could broaden latitudinal width.

Appendix A: Detailed Derivation of Diffusion Coefficients

Formulation of the bounce resonance diffusion coefficients utilizes a set of relativistic particle equations from Bortnik and Thorne (2010) and Chen et al. (2015) as follows:

$$\frac{\mathrm{d}p_z}{\mathrm{d}t} = -\frac{p_\perp^2}{2\gamma mB}\frac{\mathrm{d}B}{\mathrm{d}s} + g(\lambda)\sum_n \left[e^{i\phi_n}\frac{qE_{zn}J_0(\beta_n) + iqv_\perp B_{xn}J_{+1}(\beta_n)}{2} + \text{c.c.}\right] \tag{A1}$$

$$\frac{\mathrm{d}p_\perp}{\mathrm{d}t} = +\frac{p_z p_\perp}{2\gamma mB}\frac{\mathrm{d}B}{\mathrm{d}s} + g(\lambda)\sum_n \left[e^{i\phi_n}\frac{-iqE_{yn} - iqv_z B_{xn}}{2}J_{+1}(\beta_n) + \text{c.c.}\right] \tag{A2}$$

$$\dot{\phi}_n = -\omega_n + k_{zn}v_z \tag{A3}$$

Here m is the electron's mass, γ is the Lorentz factor, and p_z (v_z) and $p_\perp$ ($v_\perp$) are the particle's parallel and perpendicular momentum (velocity), respectively. Our background field B is assumed to be dipolar and s is the distance along the background field from the geomagnetic equator. E_z, E_y, and B_x are magnetosonic wave electromagnetic field components in the field-aligned coordinate system where z is along the background field, x-z plane contains the wave vector $\vec{k}$, and y completes the right-handed coordinate system. The terms $J_0(\beta)$ and $J_{+1}(\beta)$ are Bessel functions of the first kind with argument $\beta_n = \frac{k_{\perp n}p_\perp}{qB}$, where n denotes the nth wave, $k_{\perp n}$ is the corresponding perpendicular wave number, and q is the charge of an electron. The term "c.c." is the complex conjugate of the wave terms. These Bessel terms arise as a consequence of the gyrophase average over gyromotions of finite Larmor radius, which is also known as the finite Larmor radius effect. The factor $g(\lambda) = \exp(-\frac{\lambda^2}{\Delta\lambda^2})$ represents a realistic latitudinal profile of the wave amplitude, where $\Delta\lambda$ is the distribution width of the wave amplitude. The term $\dot{\phi}_n$ denotes the wave phase seen by the center of the gyromotion, ω_n is the wave's angular frequency, and k_{zn} is the field-aligned component of the wave vector. The set of equations can be reduced to the typical guiding center approximation by letting $\beta \to 0$. The finite β leads to a weaker electric and magnetic force in the parallel direction (equation (A1)) and also causes the change in the magnetic moment μ (equation (A2)), where $\mu = p_\perp^2/2mB$. It can be shown that p^2 ($=p_\perp^2 + p_\parallel^2$) and μ are conserved without wave forces. The zero-order bounce motion without wave forces can be represented as $z = z_m \sin\theta$, and therefore, $p_z \doteq \dot{z}\gamma m = \gamma m z_m \Omega_b \cos\theta$ where $\theta = \Omega_b t + \theta_0$ is the particle bounce phase ($\dot{\theta} = \Omega_b$), z_m is the arc distance of the mirror location to the magnetic equator along the field line, Ω_b is the angular bounce frequency, and θ_0 is initial bounce phase of the particle. Similarly, $\lambda = \lambda_m \sin(\Omega_b t + \theta_0)$, where λ_m is the magnetic latitude of the particle's mirror point.

Manipulation of equations (A1) and (A2) yields $\frac{\mathrm{d}p^2}{\mathrm{d}t}$.

$$\frac{\mathrm{d}p^2}{\mathrm{d}t} = \sum_n \left[e^{i\phi_n}\left[qE_{zn}J_{0(n)}(\gamma m z_m \Omega_b)\cos\theta - iqE_{yn}J_{+1}(\beta_n)p_\perp\right] + \text{c.c.}\right] \tag{A4}$$

and

$$\frac{\mathrm{d}\mu}{\mathrm{d}t} = \sum_n e^{i\phi_n}\frac{\mu}{p_\perp}\left(-iqE_{yn} - iq(z_m\Omega_b\cos\theta)B_{xn}\right)J_{+1}(\beta_n) + \text{c.c.} \tag{A5}$$

where $\phi_n = -\omega_n t + k_{zn}z + \phi_{n0}$. ϕ_{n0} denotes initial wave phase of the nth wave at the equator.

Using the zero-order motion, we evaluate the change of p^2 and μ (Δp^2 and $\Delta\mu$) up to the first order over a bounce period τ due to the presence of waves by integrating equations (A4) and (A5). We note that integrating equations (A4) and (A5) only require integration of the factors of $e^{i\phi_n}g(\lambda)$ and $e^{i\phi_n}g(\lambda)\cos\theta$ over a bounce period. Making use of the two transformations: $\exp(iz\sin\theta) = \sum_{l_1=-\infty}^{\infty} J_{l_1}(z)\exp(il_1\theta)$ and $\exp(a\cos 2\theta) = \sum_{k_2=-\infty}^{\infty} I_{k_2}(a)\cos(2k_2\theta)$, we have the integrals

$$\int_0^{\tau_b} \mathrm{d}te^{i\phi_n}g(\lambda) = \sum_n \tau_b e^{(i\phi'_{n0})} \sum_{l_1}\sum_{k_2} J_{l_1}(k_{zn}z_m)I_{k_2}(c_0)e^{-c_0}\frac{1}{2}\delta(l_1 - x_n \pm 2k_2) \tag{A6}$$

and

$$\int_0^{\tau_b} \mathrm{d}te^{i\phi_n}g(\lambda)cos\theta = \sum_n \tau_b e^{(i\phi'_{n0})} \sum_{l_1}\sum_{k_2} J_{l_1}(k_{zn}z_m)I_{k_2}(c_0)e^{-c_0} \times \frac{1}{4}\delta(l_1 - x_n \pm 2k_2 \pm 1) \tag{A7}$$

where $c_0 = \lambda_m^2/2\Delta\lambda^2$, $(1/2\pi)\int_{\theta_0}^{2\pi+\theta_0} \mathrm{d}\theta e^{in\theta} = \delta(n)$, $x_n = \omega_b/\Omega_b$, and $\phi'_{n0} = \phi_{n0} + \frac{\omega_n}{\Omega_b}\theta_0$. As for c_0, λ_m is the magnetic latitude of the bounce mirror point and $\Delta\lambda$ is the latitudinal width of the wave power. The J_{l_1} term arises due to the dependence of the wave phase along the bounce path, $I_{k_2}(c_0)e^{-c_0}$ arises due to the Gaussian latitudinal distribution of the wave's power, and δ denotes the selection of bounce resonance where $x_n = \frac{\omega_n}{\Omega_b}$ must be an integer. The term $\delta(l_1 - x_n \pm 2k_2) = \delta(l_1 - x_n + 2k_2) + \delta(l_1 - x_n - 2k_2)$. Similarly, $\delta(l_1 - x_n \pm 2k_2 \pm 1) = \delta(l_1 - x_n + 2k_2 + 1) + \delta(l_1 - x_n - 2k_2 + 1) + \delta(l_1 - x_n + 2k_2 - 1) + \delta(l_1 - x_n - 2k_2 - 1)$.

After tedious algebra, we find

$$\begin{aligned}\Delta p^2 = &\sum_n \tau_b \exp(i\phi'_{n0}) \sum_{l_1}\sum_{k_2} J_{l_1}(k_{zn}z_m)I_{k_2}(c_0)e^{-c_0} \\ &\times \left[(-iqE_{yn}J_{+1}p_\perp)\frac{1}{2}\delta(l_1 - x_n \pm 2k_2) + (\gamma m z_m \Omega_b q E_{zn}J_0)\frac{1}{4}\delta(l_1 - x_n \pm 2k_2 \pm 1)\right] + \text{c.c.}\end{aligned} \tag{A8}$$

and

$$\begin{aligned}\Delta\mu = &\sum_n \tau_b \exp(i\phi'_{n0}) \sum_{l_1}\sum_{k_2} J_{l_1}(k_{zn}z_m)I_{k_2}(c_0)e^{-c_0} \\ &\times \left[\left(-i\frac{\mu}{p_\perp}qE_{yn}J_{+1}\right)\frac{1}{2}\delta(l_1 - x_n \pm 2k_2) + \left(i\frac{\mu}{p_\perp}qz_m\Omega_b B_{xn}J_{+1}\right)\frac{1}{4}\delta(l_1 - x_n \pm 2k_2 \pm 1)\right] + \text{c.c.}\end{aligned} \tag{A9}$$

We now have the tools to derive expressions for the change in equatorial pitch angle, $\Delta\alpha_{eq}$, and energy, ΔE, which will be used to solve the diffusion coefficients. To solve these, we use expressions for the change in both magnetically oriented momentum components $\Delta p_{\perp eq}$ and $\Delta p_{\parallel eq}$. Making note of the fact that $\tan(\alpha_{eq}) = \frac{p_{\perp eq}}{p_{\parallel eq}}$ and $\Delta E = \Delta\gamma mc^2$, where $\gamma^2 = 1 + \frac{p^2}{m^2c^2}$, we have

$$\Delta\alpha_{eq} = \frac{1}{2}\tan(\alpha_{eq})\left(\frac{\Delta\mu}{\mu} - \frac{\Delta p^2}{p^2}\right) \tag{A10}$$

and

$$\Delta E = \frac{\Delta p^2}{2\gamma m} \tag{A11}$$

To solve for the diffusion coefficient, we consider two general variables in the following forms similar to equations (A8) and (A9): $\Delta a = \tau_b \exp(i\phi'_{n0})A + \text{c.c.}$, and $\Delta b = \tau_b \exp(i\phi'_{n0})B + \text{c.c.}$, where A and B are complex numbers independent of ϕ_{n0} and θ_0, and therefore, ϕ'_{n0}. The cross diffusion term between a and b, D_{ab}, is defined as

$$\begin{aligned}D_{ab} = \left\langle\frac{(\Delta a)(\Delta b)}{2\tau_b}\right\rangle_{\phi'_{n0}} &= \frac{\tau_b}{2}\left\langle\left(A\exp(i\phi'_{n0}) + \text{c.c.}\right)\left(B\exp(i\phi'_{n0}) + \text{c.c.}\right)\right\rangle_{\phi'_{n0}} \\ &= \tau_b\left[\Re\left(AB^*\right)\right]\end{aligned} \tag{A12}$$

where $\langle\rangle$ represents the average over the initial phase ϕ'_{n0}. Note that the quantities A and B in the equation (A12) are independent of the initial wave phase ϕ'_{n0}, linearly dependent on the wave's complex amplitudes E_{zn}, B_{xn}, and E_{yn}, and contain the harmonic selective terms $\delta(l_1 - x_n \pm 2k_2)$ and $\delta(l_1 - x_n \pm 2k_2 \pm 1)$. These equations allow us to analytically solve for $D_{\alpha_{eq}\alpha_{eq}}$, D_{EE}, and, if desired, the cross diffusion term $D_{\alpha_{eq}E}$. For example, D_{EE} requires we plug equation (A8) into (A11) to obtain ΔE. Comparing to Δa, A would be the summation terms over l_1 and k_2. After plugging into equation (A12), we can finally solve for D_{EE}.

Acknowledgments
No observational data are used for this study. We acknowledge the NSF grant 1705079 through the Geospace Environment Modeling program, the AFOSR grant of FA9550-16-1-0344, and NASA grants NNX15AF55G and NNX17AI52G.

References

Boardsen, S. A., Gallagher, D. L., Gurnett, D. A., Peterson, W. K., & Green, J. L. (1992). Funnel-shaped, low-frequency equatorial waves. *Journal of Geophysical Research*, *97*, 14,967–14,976. https://doi.org/10.1029/92JA00827

Bortnik, J., & Thorne, R. M. (2010). Transit time scattering of energetic electrons due to equatorially confined magnetosonic waves. *Journal of Geophysical Research*, *115*, A07213. https://doi.org/10.1029/2010JA015283

Cao, X., Ni, B., Summers, D., Bortnik, J., Tao, X., Shprits, Y. Y., et al. (2017). Bounce resonance scattering of radiation belt electrons by H^+ band EMIC waves. *Journal of Geophysical Research: Space Physics*, *122*, 1702–1713. https://doi.org/10.1002/2016JA023607

Cao, X., Ni, B., Summers, D., Zou, Z., Fu, S., & Zhang, W. (2017). Bounce resonance scattering of radiation belt electrons by low-frequency hiss: Comparison with cyclotron and landau resonances. *Geophysical Research Letters*, *44*, 9547–9554. https://doi.org/10.1002/2017GL075104

Chen, L., Maldonado, A., Bortnik, J., Thorne, R. M., Li, J., Dai, L., & Zhan, X. (2015). Nonlinear bounce resonances between magnetosonic waves and equatorially mirroring electrons. *Journal of Geophysical Research: Space Physics*, *120*, 6514–6527. https://doi.org/10.1029/2015JA021174

Chen, L., Thorne, R. M., Jordanova, V. K., Wang, C., Gkioulidou, M., Lyons, L., & Horne, R. B. (2010). Global simulation of EMIC wave excitation during the 21 April 2001 storm from coupled RCM-RAM-HOTRAY modeling. *Journal of Geophysical Research*, *115*, A07209. https://doi.org/10.1029/2009JA015075

Horne, R. B., Thorne, R. M., Glauert, S. A., Meredith, N. P., Pokhotelov, D., & Santolík, O. (2007). Electron acceleration in the Van Allen radiation belts by fast magnetosonic waves. *Geophysical Research Letters*, *34*, L17107. https://doi.org/10.1029/2007GL030267

Horne, R. B., Wheeler, G. V., & Alleyne, H. S. C. K. (2000). Proton and electron heating by radially propagating fast magnetosonic waves. *Journal of Geophysical Research*, *105*, 27,597–27,610. https://doi.org/10.1029/2000JA000018

Li, J., Ni, B., Ma, Q., Xie, L., Pu, Z., Fu, S., et al. (2016). Formation of energetic electron butterfly distributions by magnetosonic waves via landau resonance. *Geophysical Research Letters*, *43*, 3009–3016. https://doi.org/10.1002/2016GL067853

Li, X., & Tao, X. (2018). Validation and analysis of bounce resonance diffusion coefficients. *Journal of Geophysical Research: Space Physics*, *123*, 104–113. https://doi.org/10.1002/2017JA024506

Li, X., Tao, X., Lu, Q., & Dai, L. (2015). Bounce resonance diffusion coefficients for spatially confined waves. *Geophysical Research Letters*, *42*, 9591–9599. https://doi.org/10.1002/2015GL066324

Liu, K., Gary, S. P., & Winske, D. (2011). Excitation of magnetosonic waves in the terrestrial magnetosphere: Particle-in-cell simulations. *Journal of Geophysical Research*, *116*, A07212. https://doi.org/10.1029/2010JA016372

Ma, Q., Li, W., Thorne, R. M., & Angelopoulos, V. (2013). Global distribution of equatorial magnetosonic waves observed by THEMIS. *Geophysical Research Letters*, *40*, 1895–1901. https://doi.org/10.1002/grl.50434

Ma, Q., Li, W., Thorne, R. M., Bortnik, J., Kletzing, C. A., Kurth, W. S., & Hospodarsky, G. B. (2016). Electron scattering by magnetosonic waves in the inner magnetosphere. *Journal of Geophysical Research: Space Physics*, *121*, 274–285. https://doi.org/10.1002/2015JA021992

Maldonado, A. A., Chen, L., Claudepierre, S. G., Bortnik, J., Thorne, R. M., & Spence, H. (2016). Electron butterfly distribution modulation by magnetosonic waves. *Geophysical Research Letters*, *43*, 3051–3059. https://doi.org/10.1002/2016GL068161

Němec, F., Santolík, O., Gereová, K., Macúšová, E., de Conchy, Y., & Cornilleau-Wehrlin, N. (2005). Initial results of a survey of equatorial noise emissions observed by the Cluster spacecraft. *Planetary and Space Science*, *53*, 291–298. https://doi.org/10.1016/j.pss.2004.09.055

Roberts, C. S., & Schulz, M. (1968). Bounce resonant scattering of particles trapped in the Earth's magnetic field. *Journal of Geophysical Research*, *73*(23), 7361–7376.

Russell, C. T., Holzer, R. E., & Smith, E. J. (1969). OGO 3 observations of ELF noise in the magnetosphere. 1. Spatial extent and frequency of occurrence.*Journal of Geophysical Research*, *74*, 755–777. https://doi.org/10.1029/JA074i003p00755

Schulz, M., & Lanzerotti, L. J. (1974). *Particle diffusion in the radiation belts, physics and chemistry in space* (Vol. 7, chap. II.4, pp. 62–65). Berlin, Heidelberg: Pringer-Verlag.

Shprits, Y. Y. (2016). Estimation of bounce resonant scattering by fast magnetosonic waves. *Geophysical Research Letters*, *43*, 998–1006. https://doi.org/10.1002/2015GL066796

Shprits, Y. Y., Thorne, R. M., Horne, R. B., & Summers, D. (2006). Bounce-averaged diffusion coefficients for field-aligned chorus waves. *Journal of Geophysical Research*, *111*, A10225. https://doi.org/10.1029/2006JA011725

Sun, J., Gao, X., Chen, L., Lu, Q., Tao, X., & Wang, S. (2016a). A parametric study for the generation of ion bernstein modes from a discrete spectrum to a continuous one in the inner magnetosphere. I. Linear theory. *Physics of Plasmas*, *23*(2), 022901. https://doi.org/10.1063/1.4941283

Sun, J., Gao, X., Lu, Q., Chen, L., Tao, X., & Wang, S. (2016b). A parametric study for the generation of ion Bernstein modes from a discrete spectrum to a continuous one in the inner magnetosphere. II. Particle-in-cell simulations. *Physics of Plasmas*, *23*(2), 022902. https://doi.org/10.1063/1.4941284

Tao, X., & Li, X. (2016). Theoretical bounce resonance diffusion coefficient for waves generated near the equatorial plane. *Geophysical Research Letters*, *43*, 7389–7397. https://doi.org/10.1002/2016GL070139

Tsurutani, B. T., Falkowski, B. J., Pickett, J. S., Verkhoglyadova, O. P., Santolik, O., & Lakhina, G. S. (2014). Extremely intense ELF magnetosonic waves: A survey of polar observations. *Journal of Geophysical Research: Space Physics*, *119*, 964–977. https://doi.org/10.1002/2013JA019284

Xiao, F., Yang, C., Su, Z., Zhou, Q., He, Z., He, Y., et al. (2015). Wave-driven butterfly distribution of Van Allen belt relativistic electrons. *Nature Communications*, *6*, 8590.